

Five old open clusters more in the outer Galactic disk

Giovanni Carraro^{1,2}, Yuri Beletsky³, Gianni Marconi¹ \star

¹*European Southern Observatory, Alonso de Cordova 3107 Vitacura, Santiago de Chile, Chile*

²*Dipartimento di Astronomia, Università di Padova, Vicolo Osservatorio 3, I-35122, Padova, Italy*

³*Las Campanas Observatory, Carnegie Institution of Washington, Colina el Pino, Casilla 601, La Serena, Chile*

Submitted: June 2011

ABSTRACT

New photometric material is presented for 6 outer disk supposedly old, Galactic star clusters: Berkeley 76, Haffner 4, Ruprecht 10, Haffner 7, Haffner 11, and Haffner 15, that are projected against the rich and complex Canis Major overdensity at $225^\circ \leq l \leq 248^\circ$, $-7^\circ \leq b \leq -2^\circ$. This CCD data-set, in the UBVI pass-bands, is used to derive their fundamental parameters, in particular age and distance. Four of the program clusters turn out to be older than 1 Gyr. This fact makes them ideal targets for future spectroscopic campaigns aiming at deriving their metal abundances. This, in turn, contributes to increase the number of well-studied outer disk old open clusters. Only Haffner 15, previously considered an old cluster, is found to be a young, significantly reddened cluster, member of the Perseus arm in the third Galactic quadrant. As for Haffner 4, we suggest an age of about half a Gyr. The most interesting result we found is that Berkeley 76 is probably located at more than 17 kpc from the Galactic center, and therefore is among the most peripheral old open clusters so far detected. Besides, for Ruprecht 10 and Haffner 7, which were never studied before, we propose ages larger than 1 Gyr.

All the old clusters of this sample are scarcely populated and show evidence of tidal interaction with the Milky Way, and are therefore most probably in advanced stages of dynamical dissolution.

Key words: Open clusters and associations: general – open clusters and associations: individual: Berkeley 76, Haffner 4, Ruprecht 10, Haffner 7, Haffner 11, Haffner 15

1 INTRODUCTION

The structure and evolution of the outer Galactic disk has been the subject of intense investigation in the last years (Frinchaboy et al. 2004, Momany et al. 2006, Carraro et al. 2007a, 2010). This is because the outer disk in the anti-center direction is less dominated by confusion than other Galactic directions, a fact which renders it easier to describe its structure, and to search for signatures of ongoing or past accretion events. The latter consist of the Monoceros Ring (Chou et al. 2010 and references therein), and the Canis Major overdensity (Momany et al. 2004). However, both these structures are now considered by most researchers to be caused by the warped and flared Galactic disk (López-Corredoira et al. 2007, 2012; Carraro et al. 2008).

Among the various tracers routinely used to probe the outer disk, Galactic open clusters offer the advantage that it is relatively easy to obtain estimates of their ages and distances,

and that they are ubiquitous in the outer disk. This is a valid statement for both old and young open clusters, since the deficiency of old open clusters is most visible in the inner disk, due to the more difficult environment which prevents a cluster to survive for a long time.

In this paper we derive basic parameters of six anticenter clusters, located in the third quadrant of the Galactic disk: Berkeley 76, Haffner 4, Ruprecht 10, Haffner 7, Haffner 11, and Haffner 15 (see Table 1, where for each cluster we report Equatorial and Galactic coordinates, together with an estimate of the reddening at infinity in their direction). The rich fields they are projected against have been already studied in detail in Vázquez et al. (2008), where we highlight the properties of the conspicuous young populations we detected and use it to probe the spiral structure in that quadrant. The analysis of the clusters we performed in that paper was quite preliminary, and for this reason in this paper we are going to present the data, show the photometric diagrams, provide an extensive analysis of them, and propose updated estimates of distance and age for these clusters. In a few

\star email: gcarraro,gmarconi@eso.org, beletsky@lco.cl

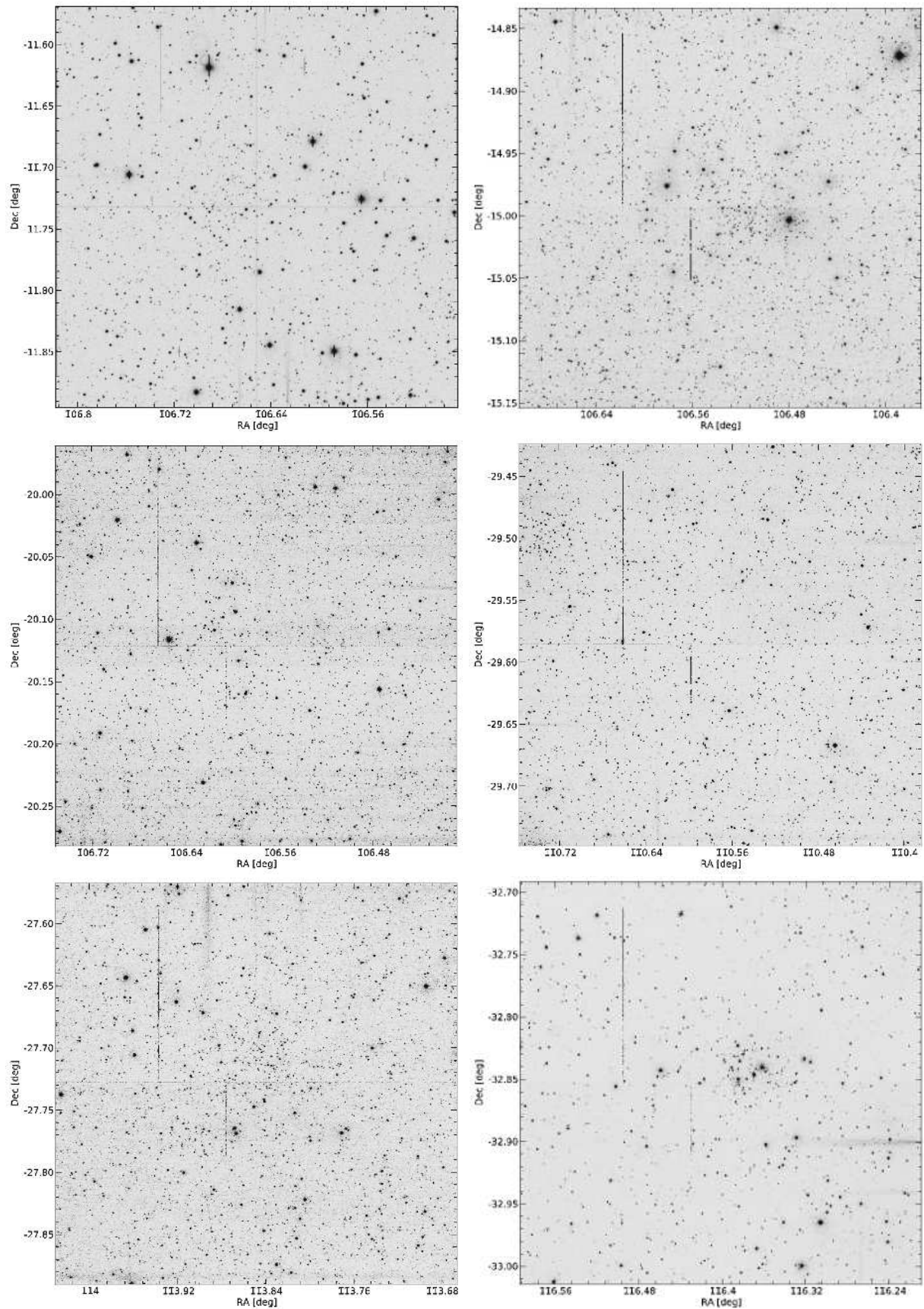


Figure 1. Montages of all CTIO CCD frames for the clusters under study. *Top row* (from left to right)- Berkeley 76, Haffner 4; *middle row* (from left to right) - Ruprecht 10, Haffner 7; *bottom row*(from left to right) - Haffner 11, Haffner 15.

Table 1. Basic parameters of the clusters under investigation. Coordinates are for J2000.0. We list also equatorial coordinates in degrees (column 4 and 5), to help the reader to look at Figs. 1 and 3. The last column reports the expected reddening along the line of sight all the way to infinity according to Schlegel et al. (1998) maps.

Name	RA	DEC	RA	DEC	l	b	$E(B-V)_\infty$
	hh : mm : ss	° : ' : "	[deg]	[deg]	[deg]	[deg]	mag
Berkeley 76	07:06:24	-11:37:00	106.60	-11.62	225.099	-1.998	0.740
Haffner 4	07:06:12	-14:59:00	106.55	-14.98	227.940	-3.586	0.721
Ruprecht 10	07:06:25	-20:05:00	106.60	-20.08	232.553	-5.854	0.645
Haffner 7	07:22:55	-29:30:00	110.73	-29.50	242.673	-6.804	0.270
Haffner 11	07:35:25	-27:43:00	113.85	-27.72	242.395	-3.544	0.824
Haffner 15	07:45:32	-32:51:00	116.38	-32.85	247.952	-4.158	1.558

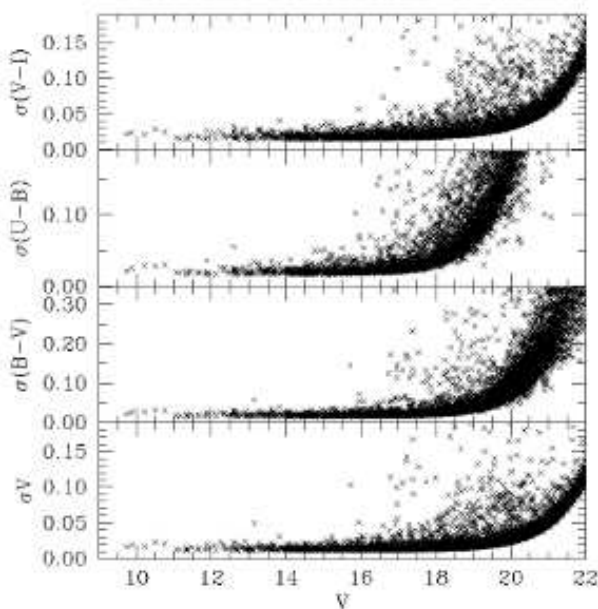


Figure 2. Trend of photometric in V, B-V, U-B and V-I as a function of V.

cases, these estimates are given for the very first time.

Interestingly enough, we anticipate that these clusters turn out to be all older than 1 Gyr, except for Haffner 5, which is a young, highly obscured cluster. This constitutes quite a useful result *per se*, since it contributes to improve the statistics of old clusters in the Galactic disk outer regions and therefore can help to provide tighter constraints for chemical evolution models aiming at recovering the chemical history and assembly of the outer disk (Carraro et al. 2007a).

The paper is organized as follows: In Section 1 we present the data, the observation strategy, and the extraction and calibration of the photometry. In the same Section, details are provided on the astrometry, completeness, and star count analysis. A summary of the information available in the literature for these clusters is presented in Section 2, while Section 3 introduces the basic diagrams we use to extract clusters' fundamental parameters. Finally, Section 4 summarizes the results and discusses their implications.

1.1 Observations and data reduction

The targets were observed with the Y4KCAM camera attached to the Cerro Tololo Inter-American Observatory (CTIO) 1-m telescope, operated by the SMARTS consortium[†] during an observation run in Nov-Dec 2005. This camera is equipped with an STA 4064×4064 CCD[‡] with 15- μ m pixels, yielding a scale of 0.289"/pixel and a field-of-view (FOV) of 20'×20' at the Cassegrain focus of the CTIO 1-m telescope. The CCD was operated without binning, at a nominal gain of 1.44 e⁻/ADU, implying a readout noise of 7 e⁻ per quadrant (this detector is read by means of four different amplifiers).

In Table 2 we present the log of our *UBVI* observations, while in Fig 1 we show astrometrized images, resulting from montaging all the available exposures and filters. All observations were carried out in photometric, good-seeing (always less than 1.2 arcsec), conditions. Our *UBVI* instrumental photometric system was defined by the use of a standard broad-band Kitt Peak *UBVI_{kc}* set of filters.[§] To determine the transformation from our instrumental system to the standard Johnson-Kron-Cousins system, and to correct for extinction, we observed stars in Landolt's areas Rubin 149, SA 95, TPhe, PG 0231(Landolt 1992) multiple times and with different air-masses ranging from ~ 1.03 to ~ 2.0 , and covering quite a large color range $-0.3 \leq (B-V) \leq 1.7$ mag.

1.2 Photometric reductions

Basic calibration of the CCD frames was done using IRAF[¶] package CCDRED. For this purpose, zero exposure frames and twilight sky flats were taken every night. Photometry was then performed using the DAOPHOT/ALLSTAR stand-alone packages. Instrumental magnitudes were extracted following the point-spread function (PSF) method

[†] <http://http://www.astro.yale.edu/smarts>

[‡] <http://www.astronomy.ohio-state.edu/Y4KCam/detector.html>

[§] <http://www.astronomy.ohio-state.edu/Y4KCam/filters.html>

[¶] IRAF is distributed by the National Optical Astronomy Observatory, which is operated by the Association of Universities for Research in Astronomy, Inc., under cooperative agreement with the National Science Foundation.

Table 2. *UBVI* photometric observations of star clusters.

Target	Date	Filter	Exposure (sec)	airmass
Haffner 15	2005 Nov 30	<i>U</i>	60, 1000	1.00–1.02
		<i>B</i>	30, 800	1.00–1.01
		<i>V</i>	15, 400	1.00–1.01
		<i>I</i>	15, 400	1.00–1.01
Haffner 4	2005 Dec 01	<i>U</i>	30, 1200	1.00–1.03
		<i>B</i>	20, 900	1.00–1.06
		<i>V</i>	15, 600	1.00–1.05
		<i>I</i>	15, 600	1.00–1.04
Haffner 11	2005 Dec 01	<i>U</i>	30, 1200	1.00–1.05
		<i>B</i>	20, 900	1.00–1.05
		<i>V</i>	15, 600	1.00–1.05
		<i>I</i>	15, 600	1.00–1.03
Berkeley 76	2005 Dec 02	<i>U</i>	30, 1200	1.05–1.08
		<i>B</i>	20, 900	1.06–1.09
		<i>V</i>	15, 600	1.07–1.08
		<i>I</i>	15, 60	1.06–1.09
Ruprecht 10	2005 Dec 03	<i>U</i>	30, 1200	1.05–1.14
		<i>B</i>	20, 720	1.06–1.17
		<i>V</i>	10, 30, 540	1.07–1.15
		<i>I</i>	10, 540	1.06–1.14
Haffner 7	2005 Dec 03	<i>U</i>	30, 1200	1.00–1.02
		<i>B</i>	20, 900	1.00–1.02
		<i>V</i>	15, 600	1.00–1.01
		<i>I</i>	15, 300	1.00–1.01

(Stetson 1987). A quadratic, spatially variable, master PSF (PENNY function) was adopted, because of the large field of view of the two detectors. Aperture corrections were then determined in each image by performing aperture photometry of a suitable number (typically 10 to 20) of bright, isolated, stars in the field. Five different apertures were used, going from the small aperture used for clusters’ frame reduction (4-7 pixels, depending on the cluster) to the large one used for standard stars (14 pixels). A growth curve was then built up to estimate the correction. These total corrections were found to vary from 0.160 to 0.290 mag, depending on the filter. The PSF photometry was finally aperture-corrected, filter by filter.

1.3 Photometric calibration

During the same observing run we observed the old open cluster Auner 1 (Carraro et al. 2007b), the dwarf planet Eris (Carraro et al. 2006) and three Galactic fields centered on the Canis Major overdensity (Carraro et al. 2008). In these papers we reported the photometric calibration procedure and the various color equations, which we are not going to repeat here. The reader is referred to those papers for all the details. We only remind the reader that typical total errors combining ALLSTAR errors and calibration errors (see Patat & Carraro 2001, Appendix A1, for details) are shown in Fig 2.

1.4 Completeness and astrometry

Completeness corrections were determined by running artificial star experiments on the data. Basically, we created

several artificial images by adding artificial stars to the original frames. These stars were added at random positions, and had the same colour and luminosity distribution of the true sample. To avoid generating overcrowding, in each experiment we added up to 20% of the original number of stars. Depending on the frame, between 1000 and 5000 stars were added. In this way we have estimated that the completeness level of our photometry is better than 90% down to *V* and *I* = 20.5.

Each optical catalog was then cross-correlated with 2MASS, which resulted in a final catalog including *UBVI* and *JHK_s* magnitudes. As a by-product, pixel (i.e., detector) coordinates were converted to RA and DEC for J2000.0 equinox, thus providing 2MASS-based astrometry, useful for *e.g.* spectroscopic follow-up. The rms of the residuals in the positions were 0."17, which is about the astrometric precision of the 2MASS catalogue (0."12, Skrutskie et al. 2006).

All the data discussed in this paper will be made available at the WEBDA^{||} database maintained by E. Paunzen in Vienna and at VizierR. A sample of the data is shown in Table 3 for the case of Haffner 4.

2 LITERATURE MATERIAL

We observed all these clusters back in 2005 and at that time no studies existed in literature on them.

However, in the following years, and before the analysis presented in this paper, various studies appeared. We summarize here the basic results of these investigations.

Hasegawa et al. (2008) presented CCD BVI photometry of Berkeley 76 and Haffner 4. Their photometry is typically 3-4 magnitudes shallower than the present study and rarely reaches *V* ~ 19 mag. They found (see their Table 4) for Berkeley 76 an age of 1.6 Gyr for *Z*=0.000 metallicity, a reddening *E*(*V*-*I*)=0.70 and a corrected distance modulus (*m*-*M*)₀ = 14.39. As for Haffner 4, they found an age of 1.3 Gyr for a metallicity value of *Z*=0.008, a reddening *E*(*V*-*I*) = 0.40 and a corrected distance modulus (*m*-*M*)₀ = 13.24.

Using the 2MASS catalog, Bica & Bonatto (2005) derived estimates of the basic parameters of Haffner 11. They suggest the cluster is 0.95 Gyr old, with a reddening *E*(*B*-*V*) = 0.36 and a corrected distance modulus (*m*-*M*)₀ = 13.60. This same cluster was later studied by Piatti et al. (2009) using photometry in the Washington system. These authors find significantly different results from Bica & Bonatto (2005), proposing that Haffner 11 is 0.5 Gyr old, with a reddening *E*(*B*-*V*)= 0.57 and a corrected distance modulus (*m*-*M*)₀ = 13.90.

Finally, Haffner 15 was targeted by Paunzen et al. (2006) in their search for peculiar stars in open clusters. In their study they report an age of 15 Myr, a reddening *E*(*B*-*V*)=1.1 and a corrected distance modulus (*m*-*M*)₀ = 11.70.

^{||} <http://www.univie.ac.at/webda/navigation.html>

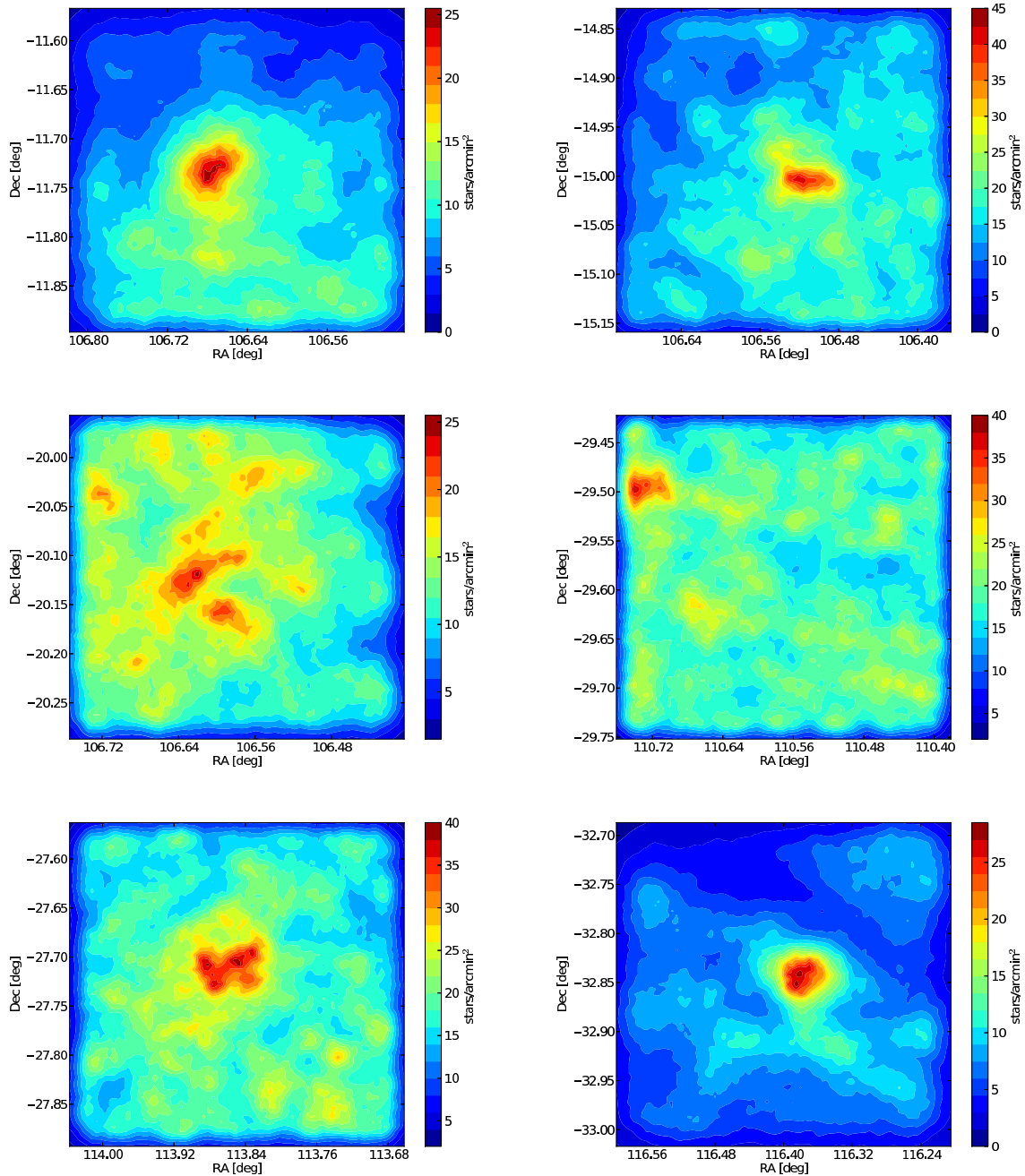


Figure 3. Contour density maps for the 6 clusters under study. *Top row* (from left to right)- Berkeley 76, Haffner 4; *middle row* (from left to right) - Ruprecht 10, Haffner 7; *bottom row*(from left to right) - Haffner 11, Haffner 15.

As for the other two clusters (Ruprecht 10 and Haffner 7), no studies exist in the literature to our knowledge.

3 CLUSTER EXISTENCE AND NATURE

Before entering into the details of the data analysis, a word of caution is in order. We are here dealing with poor stellar groups, as can be seen in the CCD images in Fig. 1. Following Platais et al. (1998), we define as a physical group or a gravitationally bound system (at odd with a random

sample of field stars), an ensemble of stars which (1) occupy a limited volume of space, (2) individually share a common space velocity, and (3) individually share the same age and chemical composition, producing distinctive sequence(s) in the Hertzsprung-Russel (H-R) diagram.

Unfortunately, we do not have kinematic information for these objects, and therefore we are going to rely on the H-R diagram and star density profiles for deciding on the nature and existence of these six stellar systems.

We start with CCD images to see what the clusters look

Table 3. A sample of the available photometric data for the star cluster Haffner 4. 99.9999 values are for not available measures.

ID	RA deg	Dec deg	U (mag)	σ_U (mag)	B (mag)	σ_B (mag)	V (mag)	σ_V (mag)	I (mag)	σ_I (mag)
1	106.3883529	-14.8720246	9.4054	0.0173	9.9289	0.1974	7.4300	0.0318	6.2286	0.0555
2	106.5810012	-14.9762229	9.2274	0.0154	9.3976	0.0157	9.2511	0.0161	9.0499	0.0516
3	106.4797390	-15.0037127	10.5342	0.0124	99.9439	99.9999	99.9999	99.9999	99.9999	99.9999
4	106.4823592	-14.9494247	10.4104	0.0119	10.5902	0.0112	10.5082	0.0114	10.3128	0.0510
5	106.4901779	-14.8493842	99.9999	99.9999	99.9999	99.9999	99.9999	99.9999	8.8061	0.0534
6	106.4469765	-14.9727220	11.2471	0.0136	11.2699	0.0120	10.7533	0.0119	10.0105	0.0512
7	106.5754512	-15.0452087	11.5660	0.0125	11.4621	0.0123	11.1297	0.0115	10.6893	0.0514
8	106.6732766	-14.8446577	12.4649	0.0218	13.3356	0.2078	10.2985	0.0329	9.1951	0.0673
9	106.5506869	-14.9631866	11.8655	0.0123	11.8413	0.0121	11.3144	0.0118	10.6159	0.0510
10	106.5745932	-14.9484442	12.0282	0.0144	11.9441	0.0129	11.3918	0.0129	10.6919	0.0510

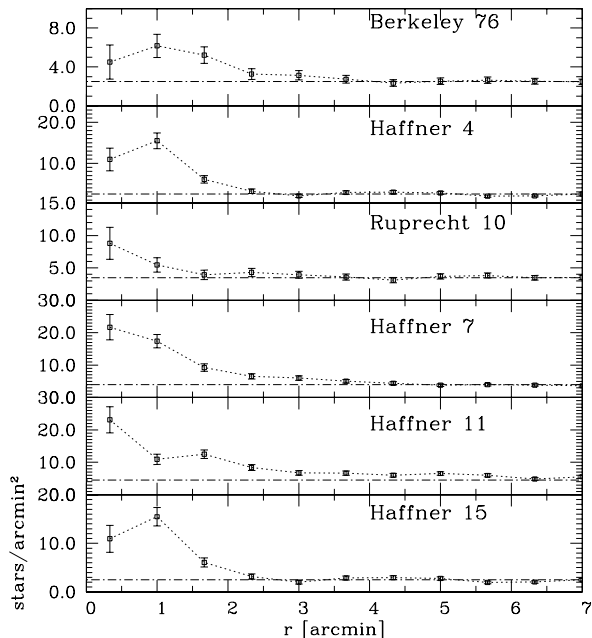


Figure 4. Radial density profiles for the 6 clusters under study.

like. By inspecting Fig 1 closely, we notice that all of them stand above the field, and fall close to the center of the Y4KCAM mosaic using catalogued coordinates (Dias et al. 2002). The only exception is Haffner 7 (mid-right image in Fig. 1) which we were forced to position in the upper-left corner of the detector to avoid the $V = 2.40$ mag η Canis Major variable star, which happens to fall less than $10'$ from Haffner 7 center. All the clusters exhibit low density against the field, which seems to indicate they are low mass, sparse objects on the verge of dissolving into the general Galactic field.

We performed star counts on the photometric datasets to derive an estimate of clusters' radial extents. These have been calculated following the same procedure described in Seleznev et al. (2010) and Carraro & Costa (2007).

Star counts and density contour maps (see Figs. 3 and 4) confirm the visual impression of CCD images, and indeed the density of stars in the cluster's area goes from only 2 to 5 times the density in the surrounding fields, as measured away from the clusters' area (see Janes & Hoq 2011 for a

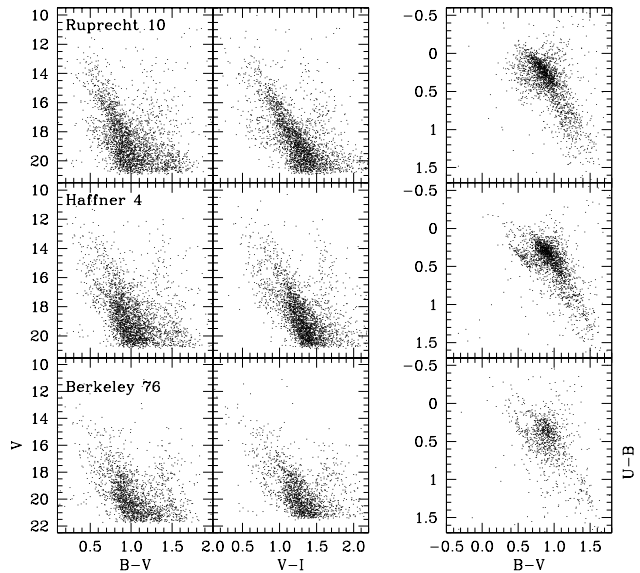


Figure 5. Color-Magnitude and Color-Color Diagrams for Berkeley 76 (lower row), Haffner 4 (mid row) and Ruprecht 10 (upper row). Only stars having error in the all the pass-bands lower than 0.05 mag are shown.

similar situation). Looking at the right columns, where the radial density profiles are shown, one can appreciate how the clusters are in fact small, with radii of the order of 2-3 arcmin only. The radius has been taken at the point where star counts reach the field level, as measured in the field far away from the cluster. The adopted radii are listed in Table 4, together with the basic parameters inferred in the next Sects. They are in agreement with the visual estimates reported in Dias et al. (2002).

We therefore conclude that all these clusters are indeed made of groups of stars spatially concentrated and standing above the general Galactic field.

Besides, looking at the middle panels of Figs. 3, where contour maps are presented, one can see how the two-dimensional structure of these clusters is far from spherical. They show elongated shapes, stretched in one or more directions, and, in some cases, with more than one density

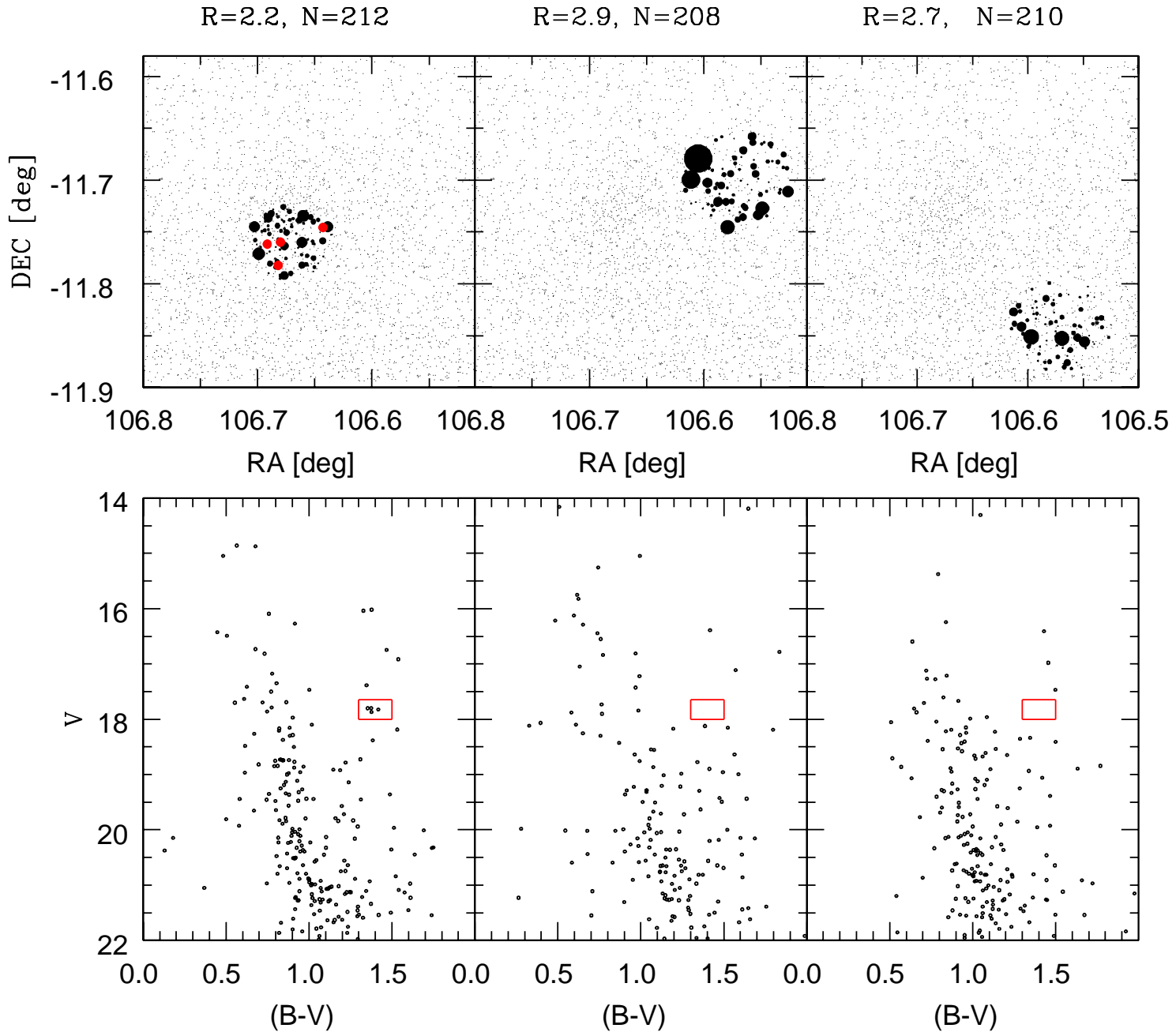


Figure 7. CMDs of Berkeley 76 and surrounding fields. Stars inside these regions are plotted with symbols proportional to their magnitude. The red box indicates the position of clump stars. These stars are plotted as red filled circles in the corresponding map.

peak in the cluster area. We are tempted to interpret these complicated structures as evidence that the clusters are undergoing dissolution due to the interaction with the Galactic environment. The ages we find for them, larger than 1 Gyr (see next Sects), confirm this fact, since the typical lifetime

for a Galactic cluster in the Milky Way is around 200 million years (Pavani & Bica 2007, Wielen 1971). The only exception - and a confirmation of this scenario - is the younger cluster Haffner 15, which looks clearly spherical. We stress, anyway, that these are qualitative conclusions driven by the

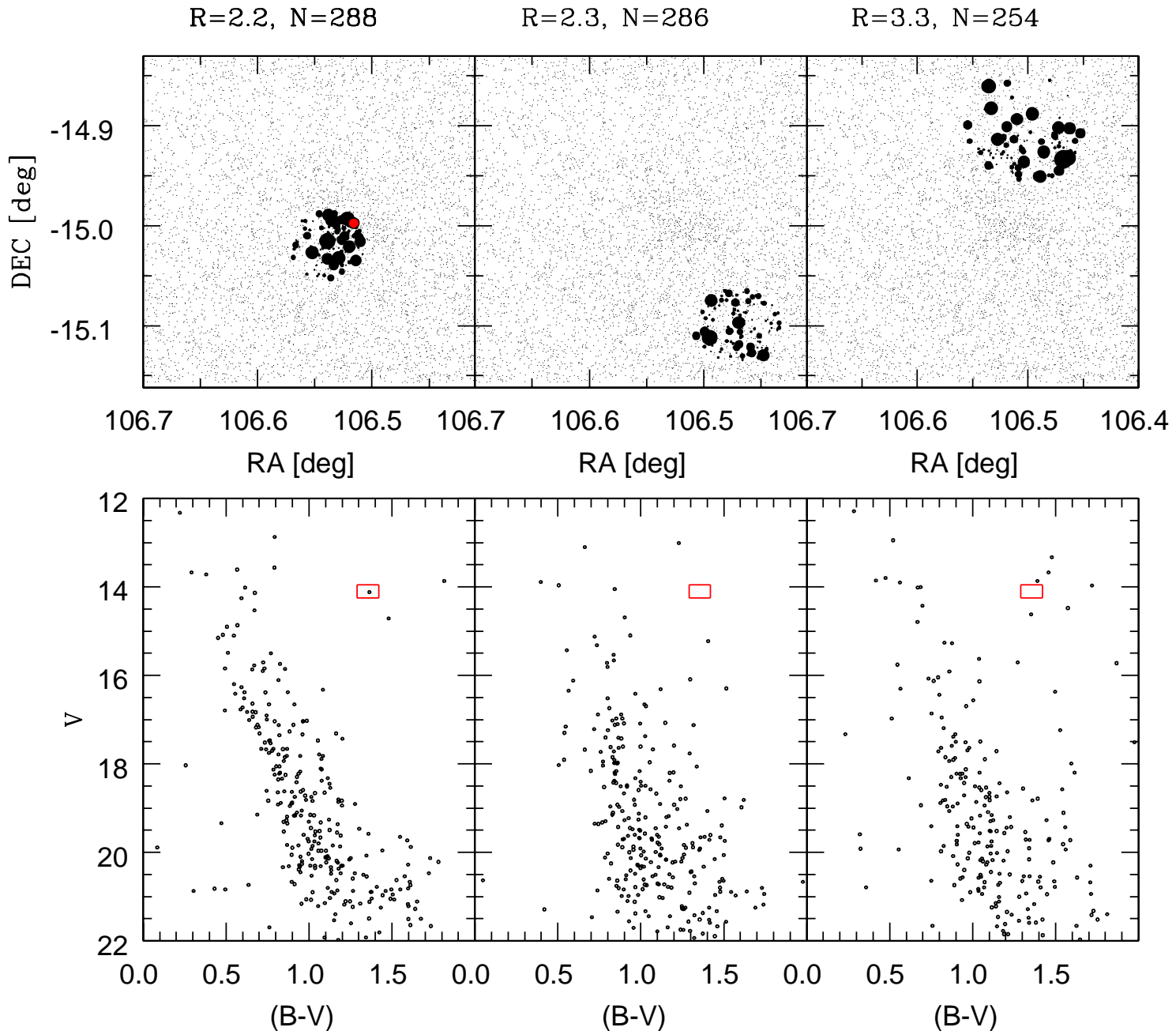


Figure 8. CMDs of Haffner 4 and surrounding fields. Stars inside these regions are plotted with symbols proportional to their magnitude. The red box indicates the position of clump stars. These stars are plotted as red filled circles in the corresponding map

photometric data only, and that a dynamical study employing radial velocities of individual stars can more firmly assess the dynamical status of these poor systems.

4 COLOR MAGNITUDE DIAGRAMS OF CLUSTERS AND SURROUNDING FIELDS

In Figs. 4 and 5 we present the Color-Magnitude (CMD) and Color-Color (CCD) diagrams of the regions containing the 6

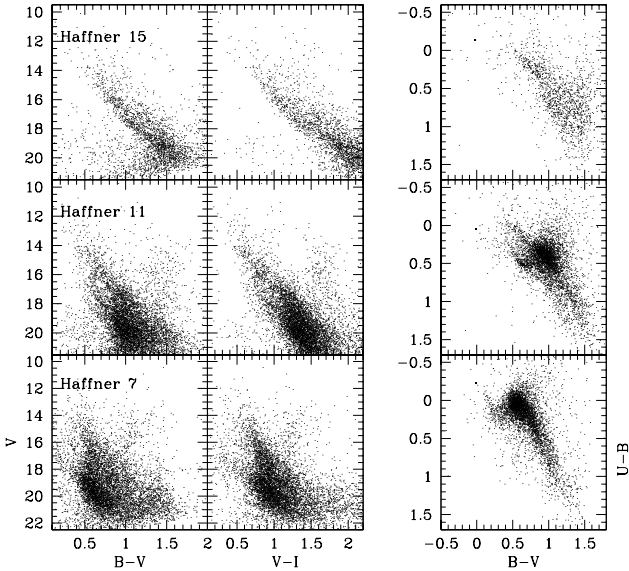


Figure 6. Color-Magnitude and Color-Color Diagrams for Haffner 7 (lower row), Haffner 11 (mid row) and Haffner 15 (upper row). Only stars having error in all the pass-band lower than 0.05 mag are shown.

clusters under study. Only stars having photometric errors lower than 0.05 mag. in all the four filters are plotted. In a wide field as the one we used (20 arcmin on a side) none of the clusters clearly emerges from the field in the CMDs, except for Haffner 15 (upper row in Fig 6). All the clusters are hidden inside a rich field star population. The latter shows the typical features of any stellar field projected toward the Canis Major overdensity, namely a *blue plume* of young stars and a prominent blue faint sequence which runs to the left of the nearby stars Main Sequence (MS) and crosses it at $16.5 \leq V \leq 18.5$, depending on the field. These features have been described and extensively interpreted *e.g.* in Carraro et al. (2008, 2010), to which we refer the reader for further details.

The aim of this paper instead is to derive the fundamental parameters of these 6 clusters, and for this reason we are going to extract photometry only for those stars which fall inside the cluster radius, as estimated in Section 1.5. This will have the effect of alleviating the field star contamination, which we expect to be significant since these lines of sight (see Table 1) are projected toward the warped thin disk (Carraro et al.2008).

We are not going to present any statistical cleaning of the clusters' CMD, since the number statistics in this clusters' sample is poor, and would generate artificial clumps and voids, which are difficult to be removed, and would complicate the interpretation of the diagrams. In the series of Figures 7 to 12, we present the CMD of each cluster and two realizations of the surrounding field, with the aim to highlight the cluster against the general field. This is possible thanks to the small size of the clusters and the wide field of our observations. In each of Figs. 6 to 11, the cluster CMD

(lower left panel) is constructed by considering all the stars falling inside a circle whose radius is close to the cluster radius, as estimated in Sect. 3. The corresponding area in the cluster map is shown in the upper left panel.

We then constructed CMDs for two different regions outside the cluster border, having about the same number of stars as the cluster region. In each figure the adopted radii are indicated together with the number of stars detected in each zone. In all cases the cluster region results to be significantly more populated than the corresponding field regions, which we needed to enlarge to include a comparable number of stars as in the cluster area.

Here below, we provide individual comments on a cluster by cluster basis.

Berkeley 76: see Fig 7. The CMD in the cluster region (left panel) shows a conspicuous main sequence (MS) which suddenly drops at $V \sim 18.8$. The bluest point is at $V \sim 19.5$, which we consider as the MS turn off point (TO). Another interesting feature is the compact group of 4 stars at $V \sim 17.9$, $B-V \sim 1.4$, which does not have any counterpart in the field, as indicated by the red box circumscribing it. These stars are plotted as red dots in the corresponding map. Their position inside the cluster region lends further support to their identification as red clump stars members to the cluster. We are going to consider this as the cluster red giant branch (RGB) clump. We believe this set of CMDs convincingly shows that we are facing a real star cluster. We shall derive estimates of its basic parameters in the next Section.

Haffner 4: see Fig 8. Also in this case the cluster CMD reveals a MS significantly more populated than in the field star CMDs. It is difficult to say where the TO is located, but we tentatively identify it at $V \sim 15.0$, $B-V \sim 0.5$. We do see a possible trace of a RGB clump in the star that we enclosed in the red box. Two redder stars can be part of the RGB as well. This star is plotted as a red dot in the corresponding map. Its position inside the cluster region lends further support to its identification as red clump star member to the cluster. We shall derive estimates of its basic parameters in the next Section.

Ruprecht 10: see Fig 9. The interpretation of Ruprecht 10 CMD is not straightforward at all. We tentatively consider as the MS the bright sequence terminating at $V \sim 14$, $B-V \sim 0.3$, while the vertical sequence terminating at $V \sim 18.5$ is produced by field stars, since it is visible also in the field star CMDs. Moreover, we consider as clump stars the 2 stars at $V \sim 14$, $B-V \sim 1.4$. These stars are plotted as red dots in the corresponding map. Their position inside the cluster region lends further support to their identification as red clump stars members to the cluster. We are going to provide estimates of the fundamental parameters in the next Section.

Haffner 7: see Fig 10. This is by far the most complicated object, because we could not cover it completely, as discussed in Sect. 3. The cluster CMD looks different from the field CMDs, and shows a clear MS. The bluest point is at

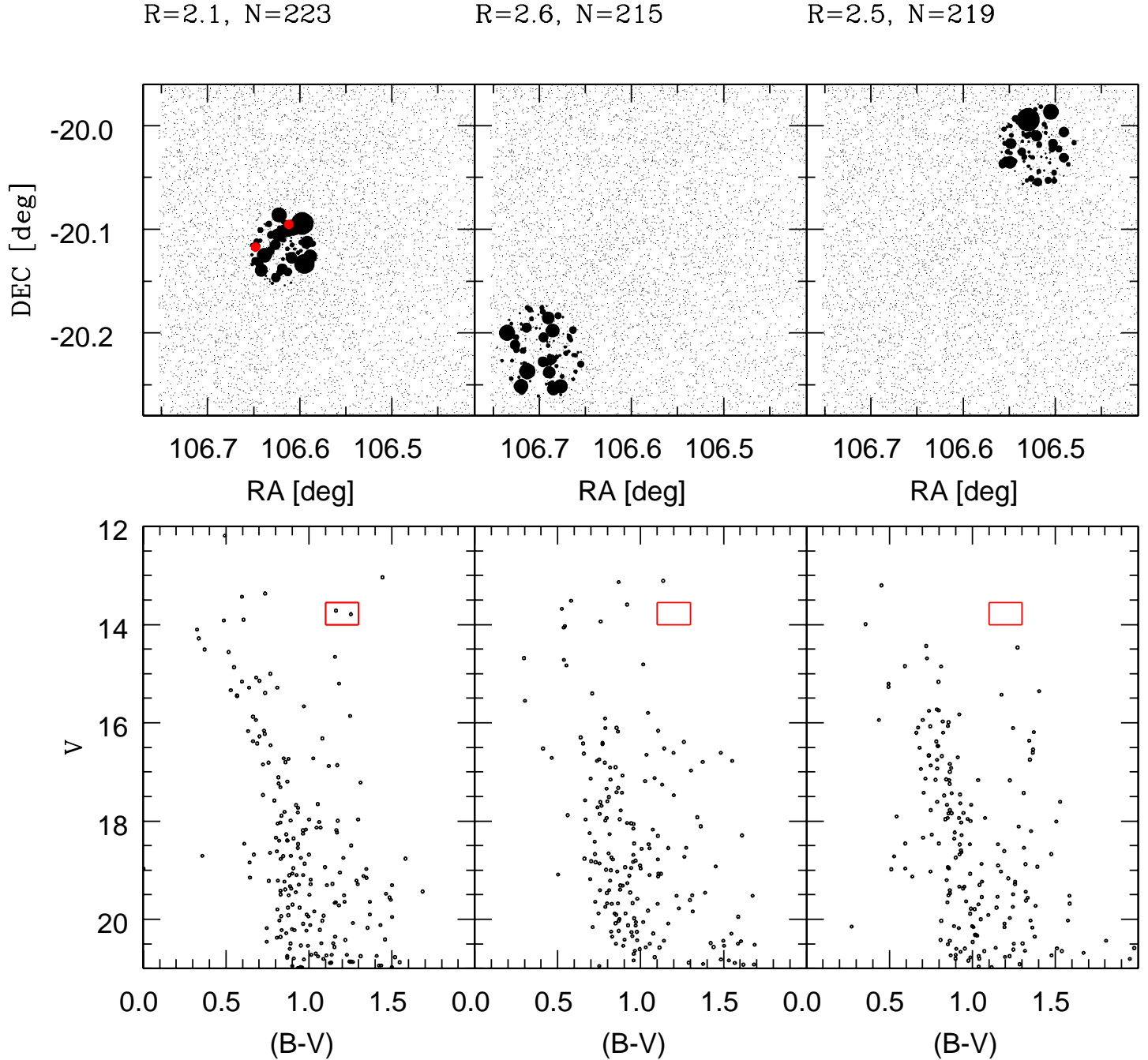


Figure 9. CMDs of Ruprecht 10 and surrounding fields. Stars inside these regions are plotted with symbols proportional to their magnitude. The red box indicates the position of clump stars. These stars are plotted as red filled circles in the corresponding map

$V \sim 16.50$, which we consider as the MS turn off point (TO). Another interesting feature is the sparse group of 4 stars at $V \sim 14.5$, $B-V \sim 1.1$, which does not have any counterpart in the field, as indicated by the red box circumscribing it. These stars are plotted as red dots in the corresponding

map. Their position inside the cluster region lends further support to their identification as red clump stars members to the cluster. We conclude that in the region of Haffner 7 there is a star concentration, and this concentration shows distinctive features in the CMD. We are going to provide es-

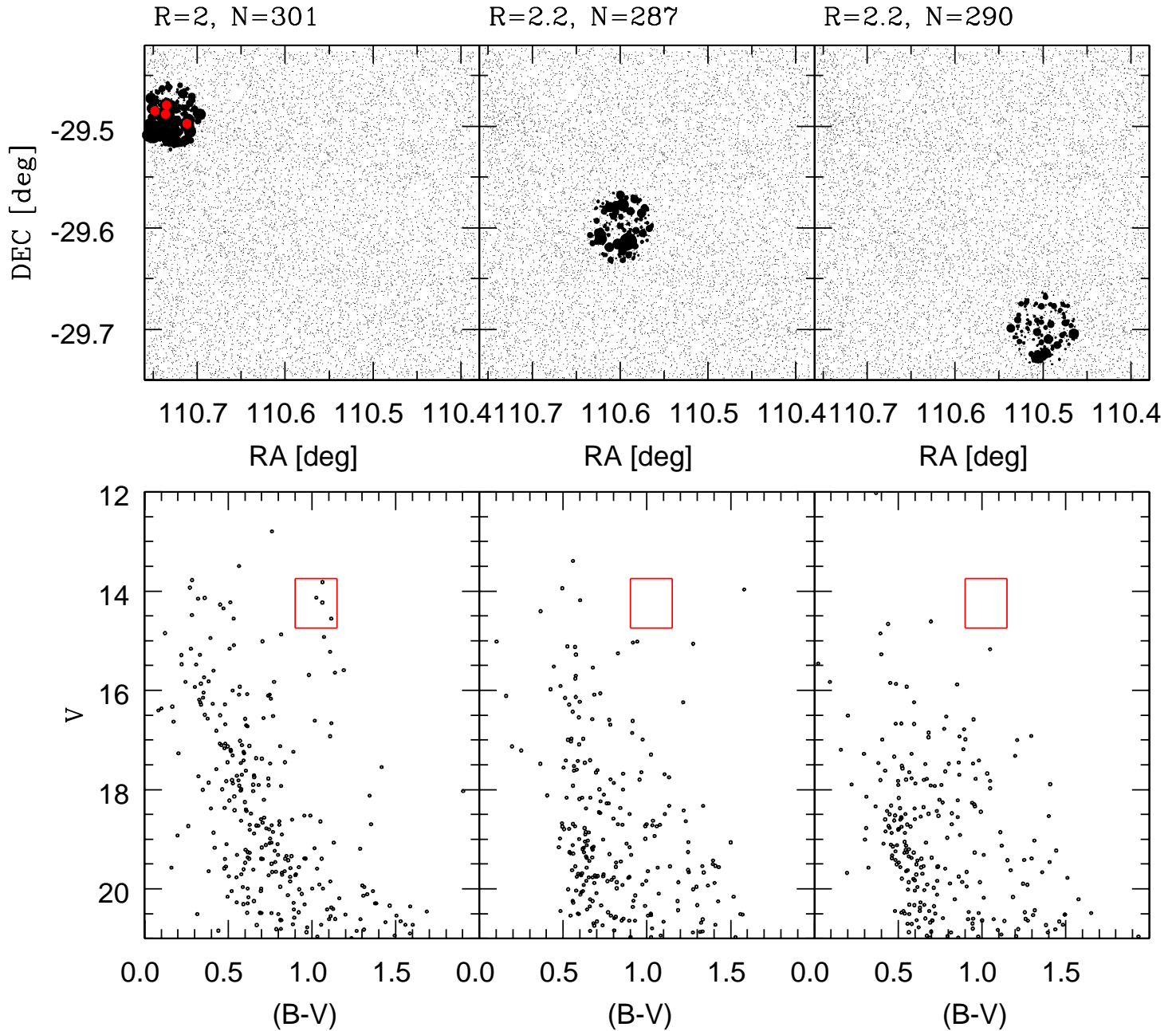


Figure 10. CMDs of Haffner 7 and surrounding fields. Stars inside these regions are plotted with symbols proportional to their magnitude. The red box indicates the position of clump stars. These stars are plotted as red filled circles in the corresponding map

timates of the fundamental parameters in the next Section.

Haffner 11: see Fig 11. This is undoubtedly a nice intermediate-age cluster, with a conspicuous clump of stars (enclosed in a red box) at $V \sim 16$, $B-V \sim 1.3$. These stars

are plotted as red dots in the corresponding map. Their position inside the cluster region lends further support to their identification as red clump stars members to the cluster. The MS TO is located at $V \sim 16.5$. The vertical sequence which drops at $V \sim 16.5$ redward of the cluster MS is produced by

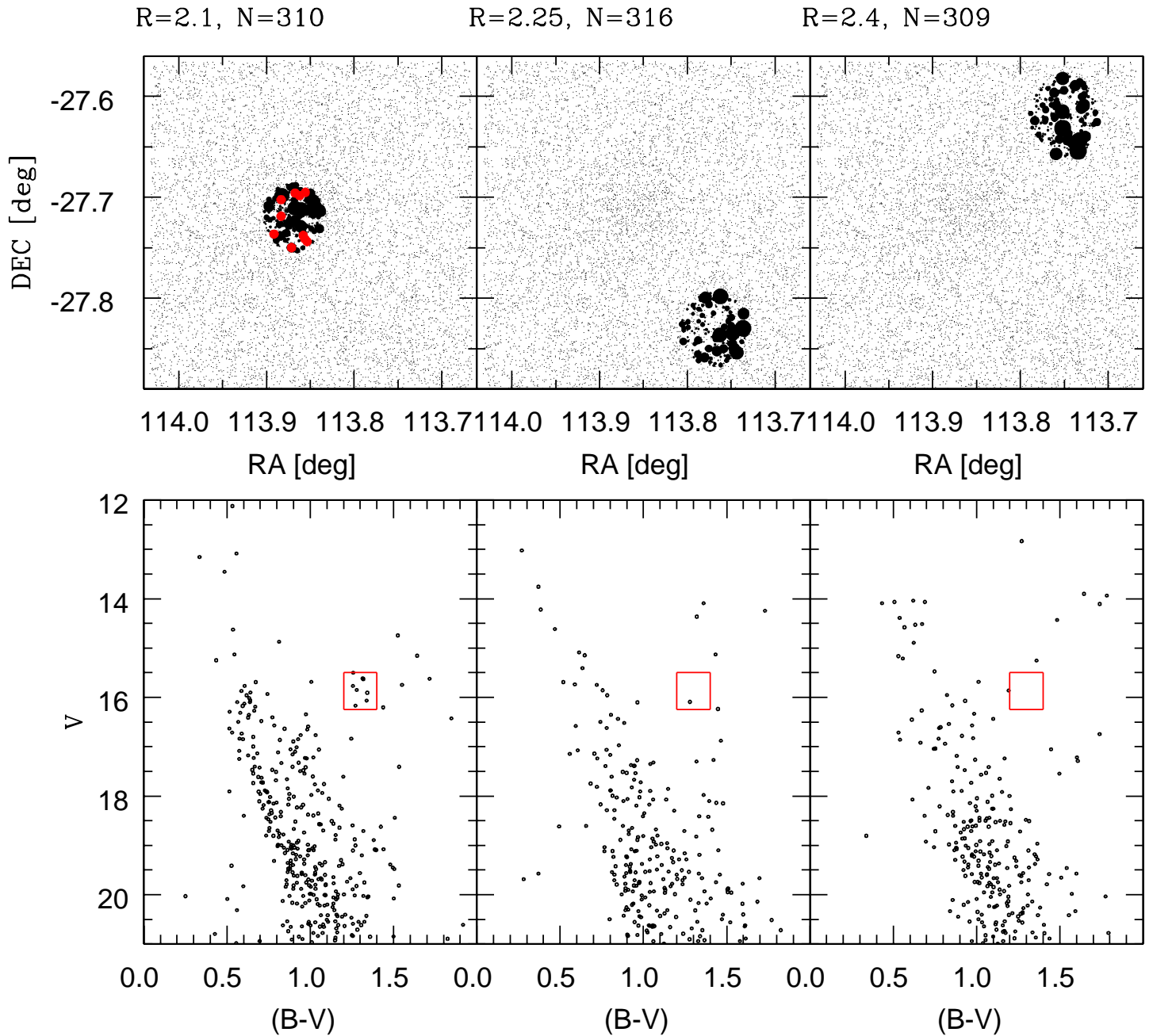


Figure 11. CMDs of Haffner 11 and surrounding fields. Stars inside these regions are plotted with symbols proportional to their magnitude. The red box indicates the position of clump stars. These stars are plotted as red filled circles in the corresponding map

the field, and appears also in the field star CMDs. Haffner 11 is the most obvious cluster amongst the ones discussed so far.

Haffner 15: see Fig 12. From the appearance of the clus-

ter area CMD we infer that Haffner 15 is a young cluster, with a TO at $V \sim 15.5$ and no indication of RGB stars. The MS is prominent and much more populated than in the field star CMDs, where the typical vertical sequence from the disk is visible. The color of the TO indicates that the

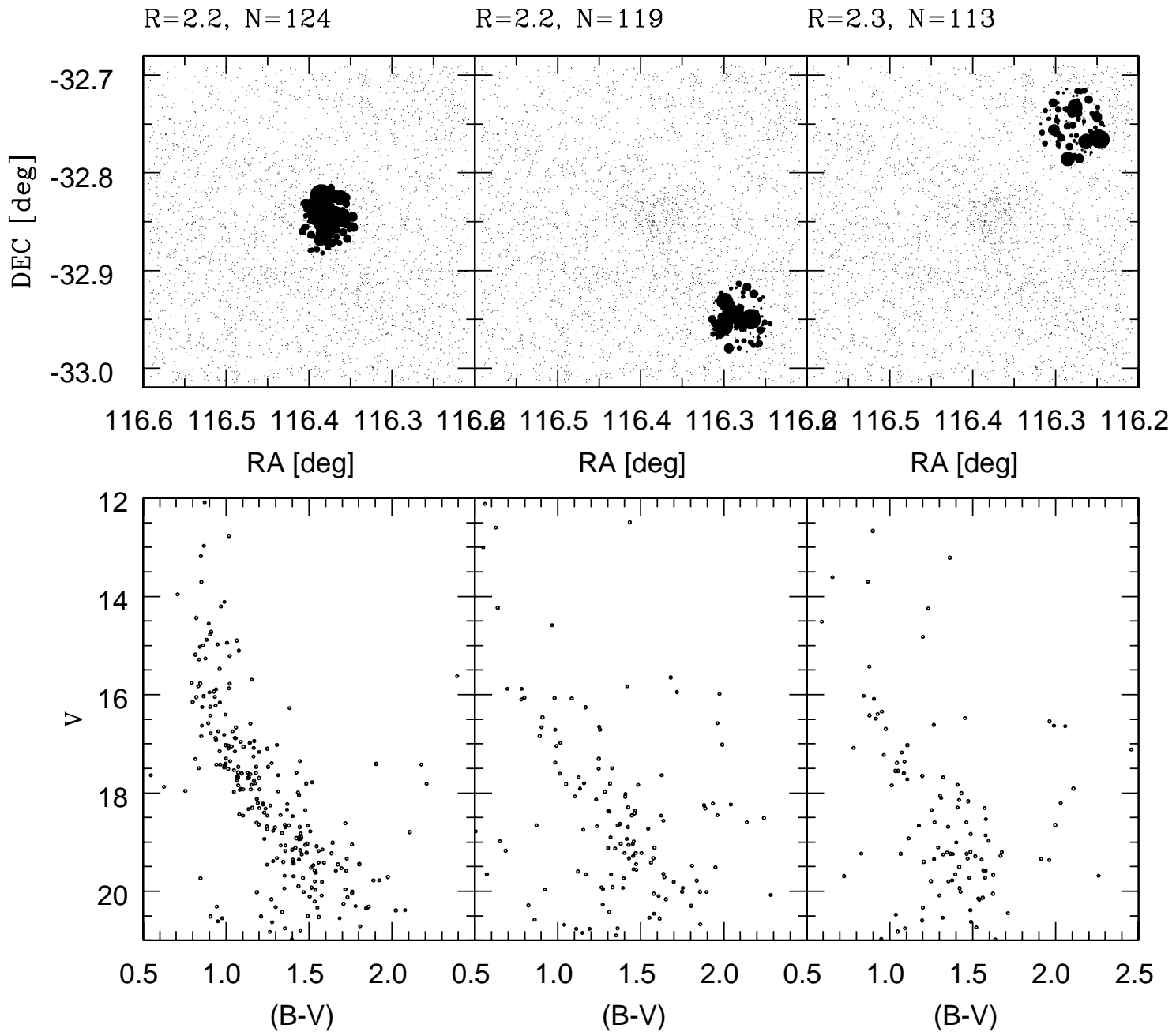


Figure 12. CMDs of Haffner 15 and surrounding fields. Stars inside these regions are plotted with symbols proportional to their magnitude.

cluster is significantly reddened. We are going to provide estimates of the fundamental parameters in the next Section.

5 DERIVATION OF CLUSTERS' BASIC PARAMETERS

The CMDs generated with only the cluster region (as defined in Sect. 1.5) stars are here compared with isochrones

extracted from the Padova suite of models (Marigo et al. 2008). This allows us to infer estimates of clusters age, distance and reddening, by assuming conservative values of the metallicity. We are fully aware that this process is highly subjective, and for this reason we consider the values we obtain as estimates, awaiting studies which can provide measures of the clusters' metal abundance.

In fact, we are here facing the well-known problem of associating reliable errors to distance and age. Without precise estimates of reddening and metallicity, it is extremely difficult to perform a proper error assessment. In theory this would imply a full error propagation which would in general produce a very large yper-volume in the parameters' space with many solutions which would not pass a simple by-eye inspection.

We will, therefore, limit ourselves to provide fitting errors for the cluster reddening and apparent distance moduli, being totally aware that they most probably are only rough lower limits awaiting improvements as soon as more precise metallicity measurements will be available. However, in deriving distance, a full propagation is done taking into account the whole range of values for reddening and distance modulus. Finally, as far as the ages is concerned, only fitting errors are reported, adopting solar metallicity (see below).

For consistency with previous studies we shall adopt 8.5 kpc as the Sun distance to the Galactic center, and 3.1 for the ratio of total to selective absorption $R_V = \frac{A_V}{E_{B-V}}$, which Moitinho (2001) demonstrated to be of general validity in this Milky Way sector.

Berkeley 76: see Fig 13

The CMDs for this cluster have been derived plotting all the stars within 2.5 arcmin from the cluster center. Still the contamination is significant, and makes the exercise of fitting an isochrone quite challenging. As previously discussed, we consider as cluster Red Giant Branch (RGB) clump the group of 4 stars at $V \sim 17.85$, $(B-V) \sim 1.35$. Such a small number of clump stars is not unusual in old open clusters, as one can see also in very recent studies (e.g. King 8 or Berkeley 23, Cignoni et al. 2011). The TO is located at $V \sim 19.5$, $(B-V) \sim 0.85$.

If we use this interpretation of the cluster CMD, we end up with an age of about 1.5 Gyr. The over-imposed - half solar ($Z=0.008$) - isochrone fits also the slope and shape of the MS. The mismatch in color for the clump is of the order of $\Delta(B-V) \sim 0.08$ mag, and can be due to a variety of reasons, like color transformations and/or mixing length calibration issues (see Carraro & Costa 2007, and Palmieri et al. 2002). We also tried solar metallicity, which does not seem suitable for an outer disk cluster, and found that for a comparable age, the fit to the MS is acceptable, but the mismatch in color with the cluster clump is much more severe.

For the adopted age and metallicity, Berkeley 76 has a reddening $E(B-V)=0.55\pm 0.1$ ($E(V-I)=0.75\pm 0.10$) and a distance modulus $(m-M)_V = 17.15 \pm 0.20$. Uncertainties in reddening and distance have been estimated by eye, shifting the isochrone along the horizontal and vertical directions, respectively, and estimating the range of values that yield acceptable fits. As a consequence, the heliocentric distance

is 12.6 kpc, and the distance from the Galactic center is 17.4 kpc, making this cluster one of the most peripheral old open cluster in the outer disk (Carraro et al. 2007).

These results are in basic agreement with Hasegawa et al. (2008), except for the distance. Looking at their results (their Fig 2) for Berkeley 76, one can indeed notice that the fit to the magnitude of the red clump is offset by almost half a magnitude, with the isochrone clump being too bright. This explains, in turn, the smaller distance in their study.

Haffner 4: see Fig 14.

As for the previous cluster, we selected only the stars inside the cluster radius (see Table 4). In this case we use solar metallicity isochrones, since the cluster is presumably located closer than Berkeley 76. Haffner 4 looks scarcely populated, and severely contaminated by field stars. The best-fit isochrone is for an age of 0.5 Gyr, which nicely follows the shape of the MS and the TO curvature, at $V \sim 15.0$, $(B-V) \sim 0.5$. No obvious indications of a red clump are present. The fit shown in Fig. 7 yields a reddening $E(B-V) = 0.50\pm 0.10$ ($E(V-I)=0.63\pm 0.10$), and a distance modulus $(m-M)_V=14.80\pm 0.15$. Once corrected, this implies a distance from the Sun of 4.4 kpc, and of 11.9 kpc from the Galactic center.

In this case our results imply an age lower than the one suggested by Hasegawa et al. (2008), and a solar metallicity.

Ruprecht 10: see Fig 15.

This cluster is sparse and has quite a distorted shape, which might indicate a stage of advanced disgregation. The MS and the evolved region of the CMD are scarcely populated. The TO is located at $V \sim 15.0$, $(B-V) \sim 0.5$, and the clump at $V \sim 14.0$, $(B-V) \sim 1.25$. By considering the stars within the cluster estimated radius, we obtained an acceptable fit for a half-solar metallicity isochrone of 1.1 Gyr, as shown in Fig. 8. This fits provides a reddening $E(B-V) = 0.28\pm 0.10$ and a distance modulus $(m-M)_V=13.40\pm 0.10$. This, in turn, yields a heliocentric distance of 2.9 kpc, and a distance from the Galactic center of 10.5 kpc.

Haffner 7: see Fig 16.

The TO is located at $V \sim 16.0$, $(B-V) \sim 0.70$, and the clump at $V \sim 14.5$, $(B-V) \sim 1.5$. By considering the stars within the cluster estimated radius, we obtained an acceptable fit for a half-solar metallicity isochrone of 1.5 Gyr, as shown in Fig. 8. This fits provides a reddening $E(B-V) = 0.13\pm 0.10$ and a distance modulus $(m-M)_V=13.65\pm 0.10$. This, in turn, yields an heliocentric distance of 4.5 kpc, and a distance from the Galactic center of 11.3 kpc.

Haffner 11: see Fig 17.

This cluster results to be a nice intermediate-age open cluster, with a well defined clump and not much contamination, when stars inside the cluster radius are isolated, and in agreement with all previous studies. It was quite an easy task to super-impose on the cluster sequence a solar metallicity isochrone for an age of 800 million years, which yields a good fit in both the CMDs. From this fit we derive a reddening $E(B-V)=0.35\pm 0.05$, and an apparent distance modulus

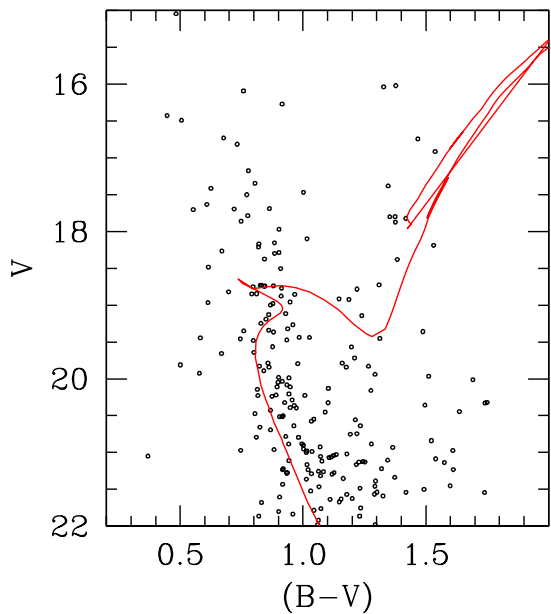


Figure 13. Isochrone solution for Berkeley 76 in the V/B-V CMD. Fitting parameters are summarized in Table 4

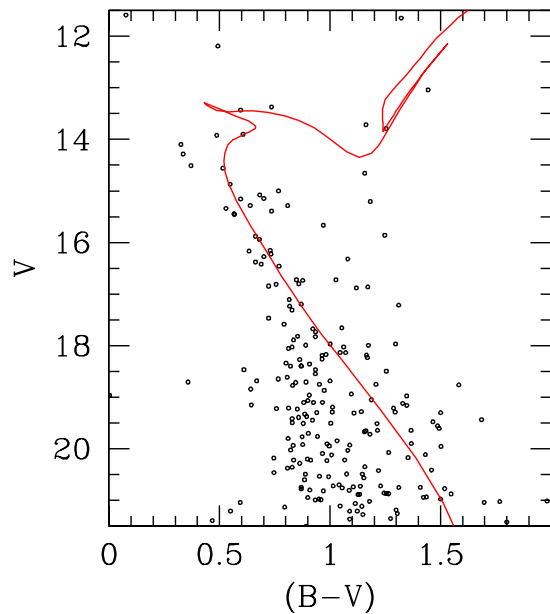


Figure 15. Isochrone solution for Ruprecht 10 in the V/B-V CMD. Fitting parameters are summarized in Table 4

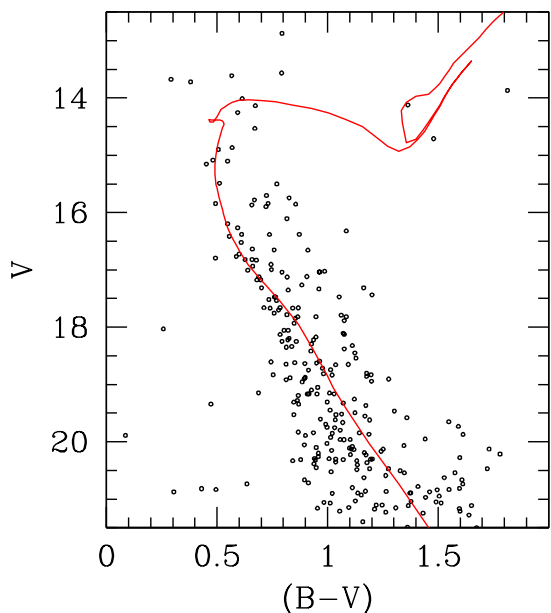


Figure 14. Isochrone solution for Haffner 4 in the V/B-V CMD. Fitting parameters are summarized in Table 4

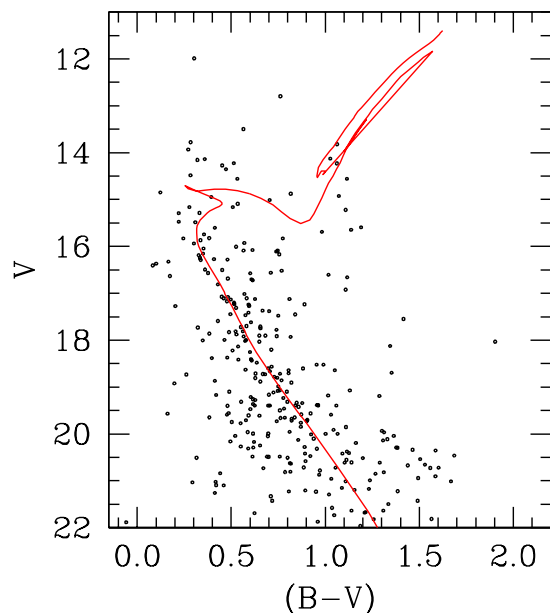


Figure 16. Isochrone solution for Haffner 7 in the V/B-V CMD. Fitting parameters are summarized in Table 4

$(m-M)_V = 15.0 \pm 0.10$. We therefore place the cluster at 6.0 kpc from the Sun, and 12.5 kpc from the Galactic center.

Our results are therefore closer to Bica & Bonatto (2005) than to Piatti et al. (2009).

Haffner 15: see Figs 18 and 19.

The preliminary estimate of the age of Haffner 15 in Vázquez et al. (2008) was 600 million years, significantly larger than the 15 Myr reported by Paunzen et al (2006). To solve this discrepancy we make use of a different set of diagrams. In detail, we make use first of the U-B/B-V color-color diagram, which is shown in Fig. 18. Here the solid line is an empirical Zero Age MS (ZAMS) from Schmidt-Kaler (1982). The same

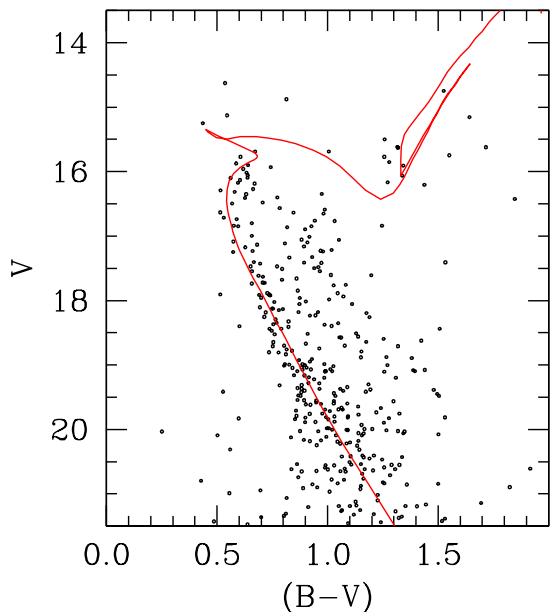


Figure 17. Isochrone solution for Haffner 11 in the V/B-V CMD. Fitting parameters are summarized in Table 4

ZAMS (dashed line) is shifted by $E(B-V) = 1.05$ along the reddening vector (indicated by the arrow in the plot) to fit the bulk of Haffner 15 stars. As justified above, we adopted a normal reddening law, which implies $R_V = 3.1$ and $E(U-B)/E(B-V) = 0.72$. To guide the eye, a few relevant spectral types are indicated, together with their displacement along the reddening path.

As a result, the cluster reddening is $E(B-V) = 1.05 \pm 0.25$, and the large dispersion indicates the cluster suffers from significant variable reddening.

We now make use of the Q method (Strayzis 1991, Carraro et al. 2010) to derive individual stars reddening, and from them compute their absolute magnitude and colors. These values are then used to build up the reddening-corrected CMDs in Fig.19, in the $(B-V)_o$ vs V_o plane (left panel), and in the $(U-B)_o$ vs V_o plane (right panel). We super-pose to the star distribution the same empirical ZAMS used before. Here the only free parameter is the distance modulus, which turns out to be $V_o - M_V = 13.00 \pm 0.10$, in both diagrams. One can better appreciate the fit in the $(U-B)_o$ vs V_o CMD, since the main sequence is more tilted in this diagram. The TO point is located at $V_o \sim 11.50$ ($V \sim 14.5$), which translates into $M_V = -1.50$. This means that the stars leaving the MS are of approximate spectral type B2, as confirmed also by inspecting the two color diagram in Fig. 11. As a consequence, one can estimate the cluster age to be around 10-20 million years (Marigo et al. 2008).

The apparent distance modulus $(m-M)_V$ is then 16.0 ± 0.10 . Overall, we therefore confirm Paunzen et al. (2006) results that Haffner 15 is indeed a young, extremely reddened open cluster. It is located 3.5 kpc from the Sun, and 10.3 kpc

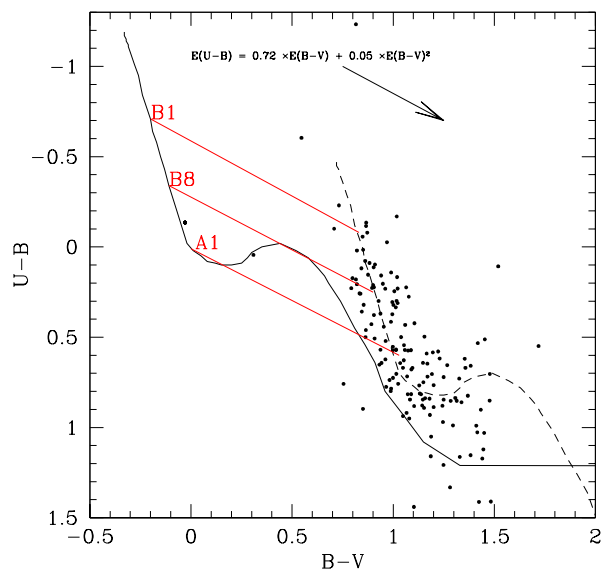


Figure 18. Two color diagrams for Haffner 15. Only stars falling inside the cluster radius are plotted. The solid line is an empirical unreddened ZAMS. The same ZAMS, shifted by $E(B-V)=1.05$ along the reddening path, is shown with a dashed line. The reddening vector for a normal reddening law is indicated with an arrow. To guide the eye, a few relevant spectral types are also indicated along the zero reddening ZAMS, together with their displacement along the reddening vector direction.

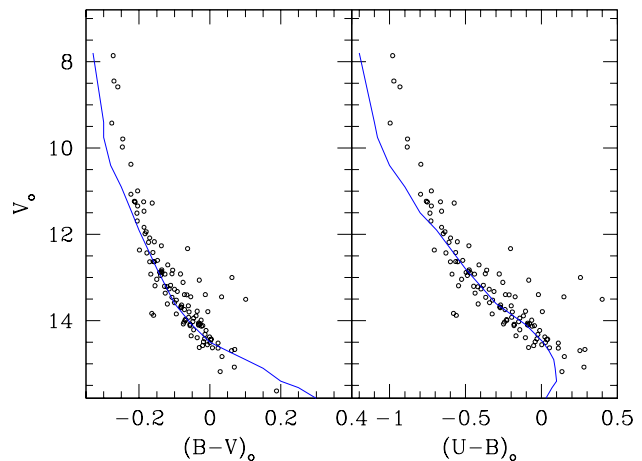


Figure 19. Reddening free CMDs in the $(B-V)_o$ vs V_o plane (left panel), and $(U-B)_o$ vs V_o plane (right panel). The solid line is a reddening free, empirical ZAMS shifted by $(V_o - M_V) = 13.00$.

from the Galactic center. Such distance is compatible with Haffner 15 membership to the Perseus arm, or to the local (Orion) arm extension in the third Galactic quadrant (Moitinho et al. 2006, Levine et al. 2006, Vázquez et al. 2008).

Table 4. Fundamental parameters estimated for the clusters. d_{\odot} indicates the distance of a cluster from the Sun, Z the height below the Galactic plane, and R_{GC} its distance to the Galactic center.

Name	Radius arcmin	E(B-V) (mag)	$(m - M)_V$ (mag)	d_{\odot} (kpc)	Age (Gyr)	Z (pc)	R_{GC} kpc
Berkeley 76	2.5±0.5	0.55±0.10	17.20±0.15	12.6	~ 1.5	~ -0.45	~ 17.4
Haffner 4	2.5±0.5	0.50±0.10	14.80±0.15	4.5	~ 0.5	~ -0.28	~ 11.9
Ruprecht 10	2.0±0.5	0.38±0.10	13.40±0.15	2.9	~ 1.1	~ -0.30	~ 10.5
Haffner 7	1.5±0.5	0.13±0.10	13.65±0.15	4.5	~ 1.5	~ -0.50	~ 11.3
Haffner 11	2.0±0.5	0.32±0.05	14.90±0.10	6.0	~ 0.8	~ -0.40	~ 12.5
Haffner 15	2.0±0.5	1.05±0.25	16.00±0.10	3.5	~ 0.02	~ -0.25	~ 10.3

6 DISCUSSION AND CONCLUSIONS

We have presented and discussed UBVI CCD photometry of six Galactic star clusters projected against the Canis Major overdensity in the third quadrant of the Milky Way: Berkeley 76, Haffner 4, Ruprecht 10, Haffner 7, Haffner 11, and Haffner 15. The fields they are immersed in have already been analysed in Vázquez et al (2008), where we searched for young diffuse stellar populations to be used as tracers of the spiral structures of the outer disk. Here we concentrated on the clusters themselves, with the goal of deriving estimates of their age and distance.

We can summarize our results as follows (see also Table 4):

- according to star counts, all the objects appear as significant overdensities with respect to the field;
- the cluster Haffner 15 is the only young object of the sample. For its age and distance it is a probable member of the Perseus arm or of the extension of the local arm into the third Galactic quadrant. This cluster is heavily and differentially reddened;
- we found one old star cluster at the extreme periphery of the disk, at a mean distance of more than 17 kpc from the Galactic center: Berkeley 76; only Saurer 1 and Berkeley 29 are located further than them (Carraro & Baume 2003);
- Ruprecht 10 and Haffner 7, two clusters that were never studied before, are found to have ages larger than 1 Gyr;
- the spatial shape of these clusters, as highlighted with star counts, may witness their dynamical status. Haffner 15, the youngest, has an almost 2-dimensional circular shape, while all the others -older than the Hyades- have complicated structures, very far from spherical. We suggest that they are close to dissolution and merging with the general Galactic field, although their actual dynamical status can only be confirmed with individual stars kinematics.

We believe this sample of clusters is quite promising, and deserves a much closer look in the future, which unfortunately GAIA will not be able to provide at those distances. The oldest, most distant clusters, in particular, are excellent targets to further probe the slope of the abundance gradient in the outer disk, and its evolution with time (Twarog et al. 1997, Carraro et al. 2007, Magrini et al. 2009).

7 ACKNOWLEDGMENT

G. Carraro would like to mention and acknowledge the great support from Cerro Tololo Observatory staff, in particular

from Edgardo Cosgrove. We thank warmly Sandy Strunk for reading the manuscript and helping us to improve the language. This study made use of the SIMBAD and WEBDA databases.

REFERENCES

- Bensby, T., Alves-Brito, A., Oey, M.S., Yong, D., Meléndez, J., 2011, *ApJ*, 735, L46
- Bica, E., Bonatto, C., 2005, *A&A*, 443, 465
- Carraro, G., Baume, G.L., 2003, *MNRAS*, 346, 18
- Carraro, G., Maris, M., Bertin, D., Parisi, M.G., 2006, *A&A*, 460, L39
- Carraro, G., Costa, E., 2007, *A&A*, 464, 573
- Carraro, G., Geisler, D., Villanova, S., Frinchaboy, P.M., Majewski, S.R., 2007a, *A&A*, 476, 217
- Carraro, G., Moitinho, A., Zoccali, M., Vázquez, R.A., Baume, G., 2007b, *AJ*, 133, 1058
- Carraro, G., Moitinho, A., Vázquez, R.A., 2008, *MNRAS*, 383, 1597
- Carraro, G., Vázquez, R.A., Costa, E., Perren, G., Moitinho, A., 2010, *ApJ*, 718, 683
- Chou, M.-Y., Majewski, S.R., Cunha, K., Smith, V.V., Patterson, R.J., Martínez-Delgado, D., 2010, *ApJ*, 720, L5
- Cignoni, M., Beccari, G., Bragaglia, A., Tosi, M., 2011, *MNRAS*, 416, 1077
- Dias, W.S., Alessi, B.S., Moitinho, A., Lépine, J.R.D., 2002, *A&A*, 389, 871
- Frinchaboy, P.M., Majewski, S.R., Crane, J.D., Reid, I.N., Rocha-Pinto, J, Phelps, R.L., Patterson, R.J., Munoz, R., 2004, *ApJ*, 620, L21
- Grocholski, A.J., Sarajedini, A., 2002, *AJ*, 123, 1603
- Hasegawa, T., Sakamoto, T., & Malasan, H. L., 2008, *PASJ*, 60, 1267
- Janes, K.A., Hoq, S., 2011, *AJ*, 141, 92
- Landolt, A.U., 1992, *AJ*, 104, 340
- Levine, E.S., Blitz, L., Heiles, C., 2006, *Science*, 312, 1773
- López-Corredoira, M., Momany, Y., Zaggia, S., Cabrera-Lavers, A., 2007, *A&A*, 472, 47
- López-Corredoira, M., Moitinho, A., Zaggia, S., Momany, Y., Carraro, G., Hammersley, P.L., Cabrera-Lavers, A., Vazquez, R.A., 2012, [arXiv:1207.2749](https://arxiv.org/abs/1207.2749)
- Magrini, L., Sestito, P., Randich, S., Galli, D., 2009, *A&A*, 494, 95
- Marigo, P., Girardi, L., Bressan, A., Groenewegen, M.A.T., Silva, L., Granato, G.L., 2008, *A&A*, 482, 883
- Moitinho, A., 2001, *A&A*, 379, 476
- Moitinho, A., Vázquez, R. A., Carraro, G., Baume, G., Giorgi, E.E., Lyra, W., 2006, *MNRAS*, 368, L77
- Momany, Y., Zaggia, S., Gilmore, G., Piotto, G., Carraro, G., Bedin, L.R., de Angeli, F., 2006, *A&A*, 451, 499

Palmieri, R., Piotto, G., Saviane, I., Girardi, L., Castellani, V.,
2002, *A&A*, 392, 115
Patat, F., Carraro, G., 2001, *MNRAS*, 325, 1591
Paunzen E., Nepotil, M., Iliev, I.Kh., Maitzen, H.M., Claret, A.,
Pintado, O.I., 2006, *A&A*, 454, 171
Pavani, D.B., Bica, E., *A&A*, 468, 139
Piatti, A.E., Clariá, J.J., Parisi, M.C., Ahumada, A.V., 2009, *New
Astronomy*, 14, 97
Platais, I., Kozhurina-Platais, V., van Leeuwen, F., 1998, *AJ*, 116,
2423
Schlegel, D.J., Finkbeiner, D.P., Davis, M., 1998, *ApJ*, 500, 525
Seleznev, A.F., Carraro, G., Costa, E., Loktin, A.V., 2010, *New
Astronomy*, 15, 61
Schmidt-Kaler Th. 1982, *Landolt-Börnstein, Numerical data and
Functional Relationships in Science and Technology, New Se-
ries, Group VI, Vol. 2(b)*, K. Schaifers and H.H. Voigt Eds.,
Springer Verlag, Berlin, p.14
Skrutskie, M. F., Cutri, R. M., Stiening, R., et al. 2006, *AJ*, 131,
1163
Stetson, P.B., 1987, *PASP*, 99, 191
Twarog, B.A., Ashman, K.M., Anthony-Twarog, B.J., 1997, *AJ*,
114, 2556
Vázquez, R.A., May, J., Carraro, G., Bronfman, L., Moitinho, A.,
Baume, G. 2008, *ApJ*, 672, 930
Wielen, R., 1971, *A&A*, 13, 309